



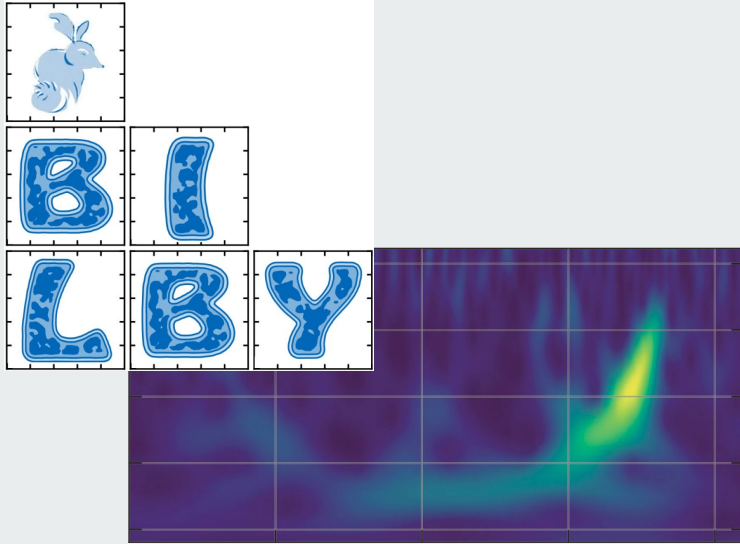
Estimation of Gravitational Wave Parameters

Jean-François Coupechoux

June 29, 2023



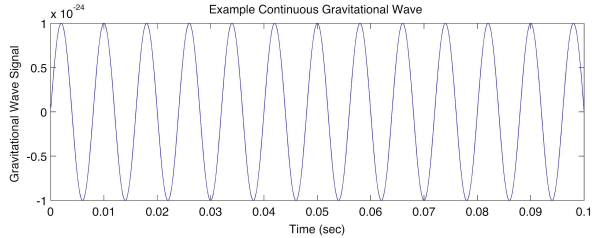
Introduction:



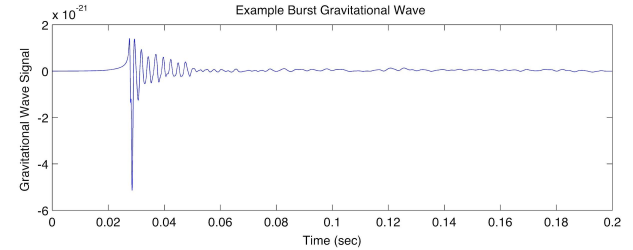
- ❖ Gravitational waves are described by Einstein's theory of general relativity (1915).
- ❖ The LIGO-Virgo-KAGRA collaboration seeks to detect gravitational waves and use them to better understand our universe.
- ❖ The detection of gravitational waves is realized thanks to a network of Michelson interferometers. First detection in 2015.

Different types of gravitational waves

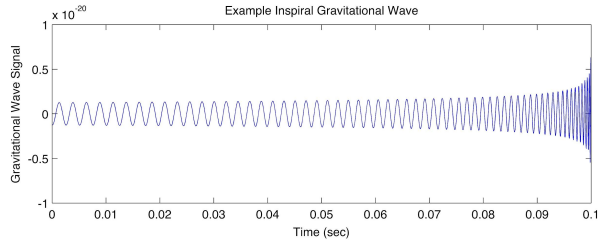
→ Continuous gravitational waves



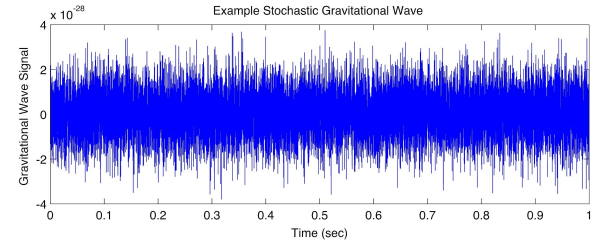
→ Burst gravitational waves



→ Inspirational gravitational waves



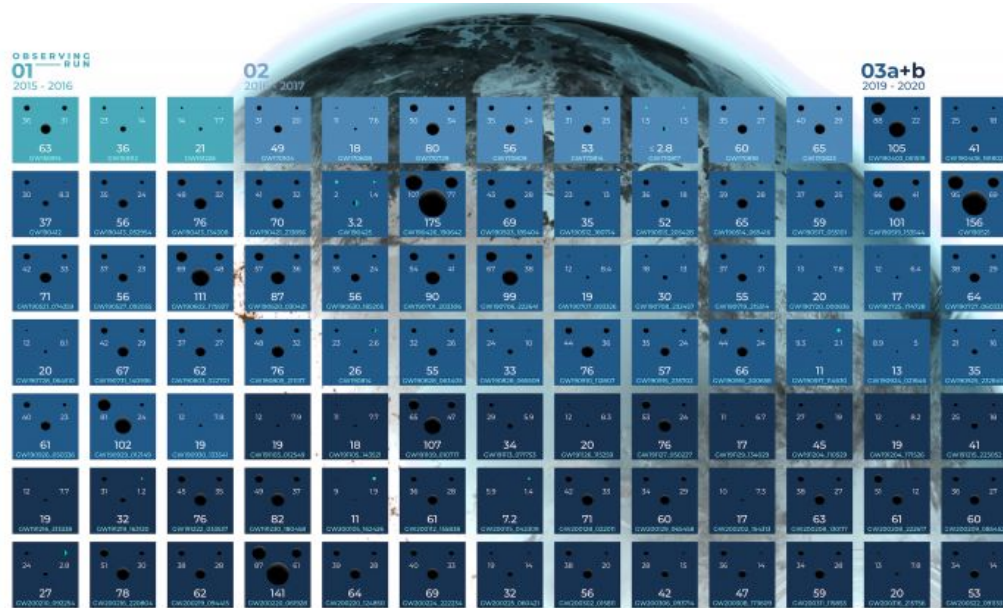
→ Stochastic gravitational waves



Bodies with spherical symmetry do not emit gravitational waves

Detections

91 events from compact binary coalescences

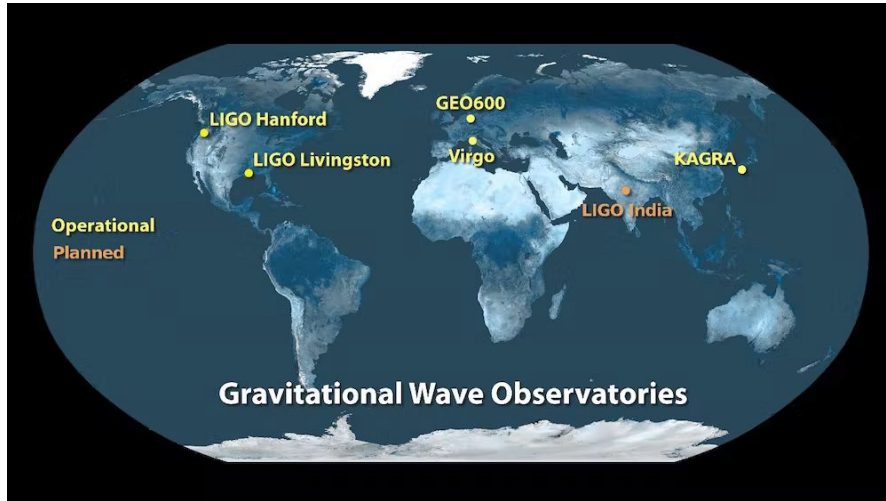


GRAVITATIONAL WAVE
**MERGER
 DETECTIONS**
 SINCE 2015

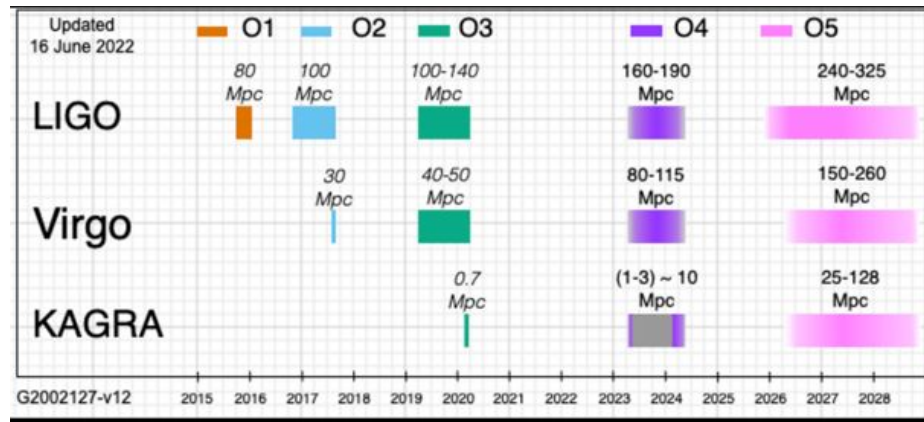
DeGrav



Detector network



O4 has started!



A network of interferometers is a necessary condition to suppress the overwhelming background by studying signal coincidences and to localize the sources by triangulation.

GraceDB Public Alerts

GraceDB Public Alerts ▾ Latest Search Alerts Pipelines Documentation Logout

Authenticated as: Viola Sordini

LIGO/Virgo/KAGRA Public Alerts

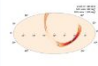

- More details about public alerts are provided in the [LIGO/Virgo/KAGRA Alerts User Guide](#).
- Retractions are marked in **red**. Retraction means that the candidate was manually vetted and is no longer considered a candidate of interest.
- Less-significant events are marked in **grey**, and are not manually vetted. Consult the [LVK Alerts User Guide](#) for more information on significance in O4.

O4 Significant Detection Candidates: **6** (7 Total - 1 Retracted)

O4 Low Significance Detection Candidates: **69** (Total)

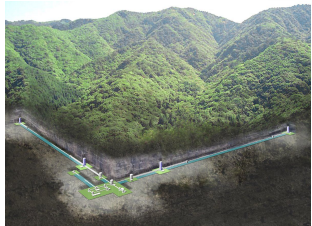
Show All Public Events

SORT: EVENT ID (A-Z) ▾

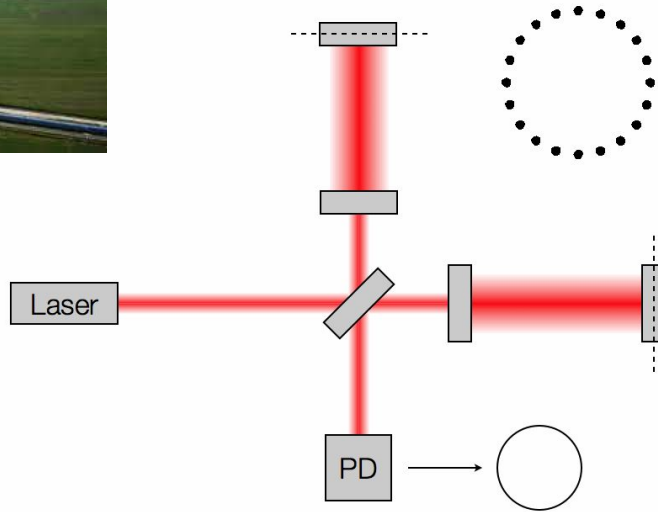
Event ID	Possible Source (Probability)	Significant	UTC	GCN	Location	FAR	Comments	Ω Scan
S230609u	BBH (96%), Terrestrial (4%)	Yes	June 9, 2023 06:49:58 UTC	GCN Circular Query Notices VOE		1 per 3.1557 years		Ω H1 Ω L1 Ω V1
S230608as	BBH (>99%)	Yes	June 8, 2023 20:50:47 UTC	GCN Circular Query Notices VOE		1 per 231.43 years		Ω H1 Ω L1 Ω V1



Amazigh Ouzriat
Morgan Lethuillier
Roberto Chierici
Viola Sordini



LIGO-Virgo-KAGRA



LMA produced the coatings used on the main mirrors of the Advanced LIGO - Virgo and KAGRA.



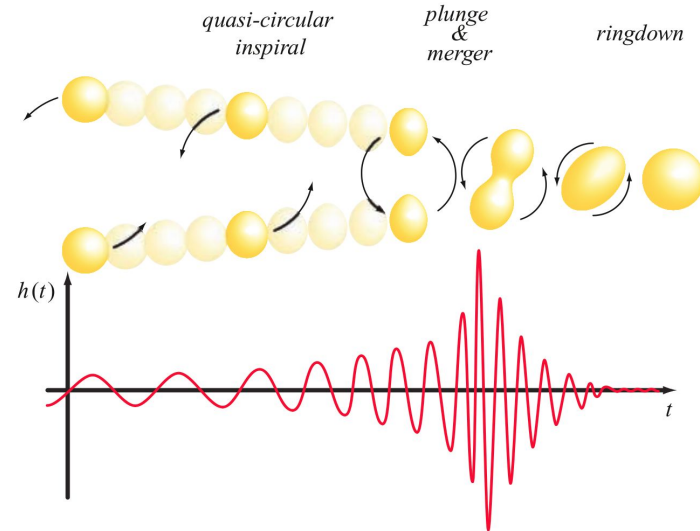
Famous events

- [GW150914](#): the first direct detection of gravitational waves
- [GW170817](#): the first detection of binary neutron star merger with electromagnetic counterpart
- [GW190521](#): two BH of 66 and 85 M_{\odot} merge to form a BH remnant of 142 M_{\odot} .
Very-high mass system!
- [GW190814](#): Coalescence of 23 M_{\odot} BH with a mystery object of 2.6 M_{\odot} .
Very asymmetric system!
- [GW200105](#) and [GW200111](#): properties consistent with neutron star–black hole binaries

Compact Binary Coalescence

Gravitational Wave-forms from compact binary coalescences

- **Inspiral phase:**
calculated by analytical expansion
- **Plunge and merge phase:**
described via numerical relativity
- **Ringdown phase phase:**
described by perturbation methods





BNS Simulations

→ Numerical Relativity

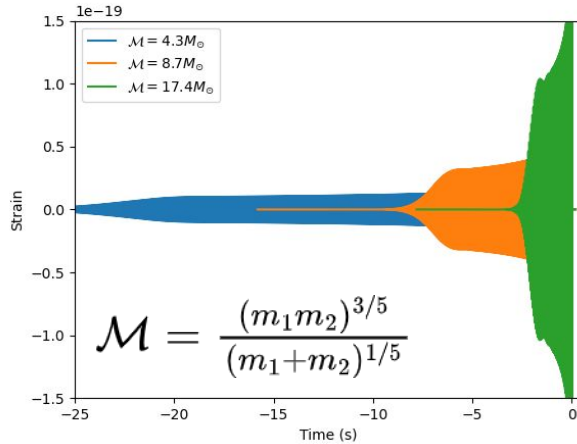
Solved using
WhiskyTHC

LS220 tabulated EoS

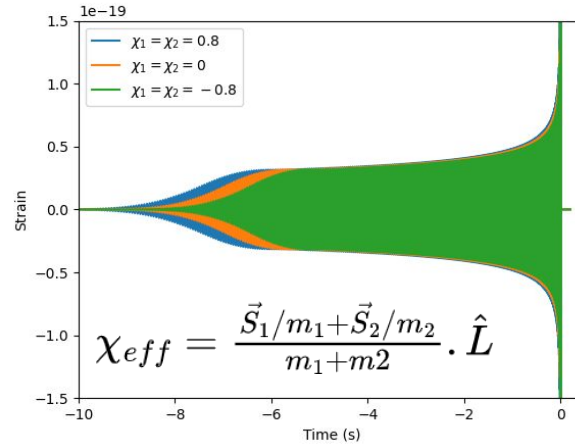
Initial condition
calculated using
LORENE with two equal
mass stars of $1.35 M_{\odot}$

Impact of intrinsic parameters

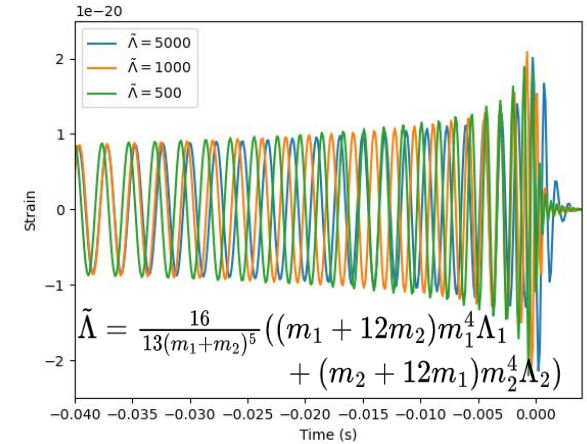
→ Masses



→ Spins

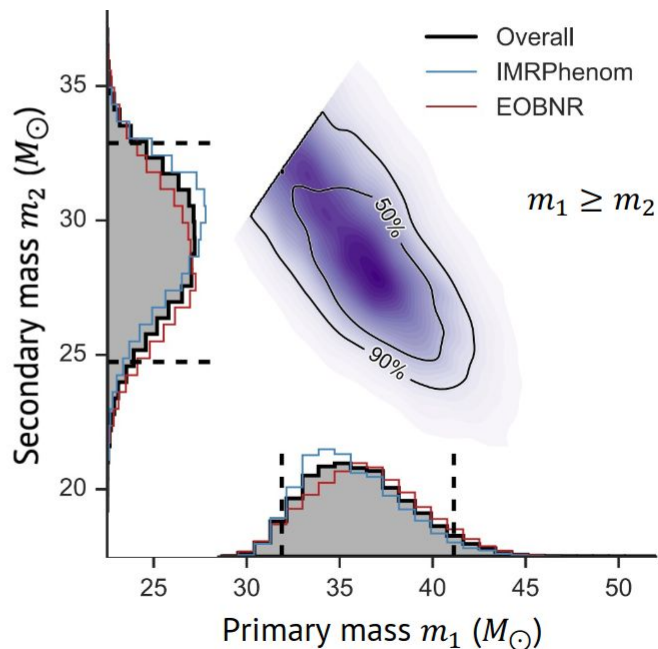
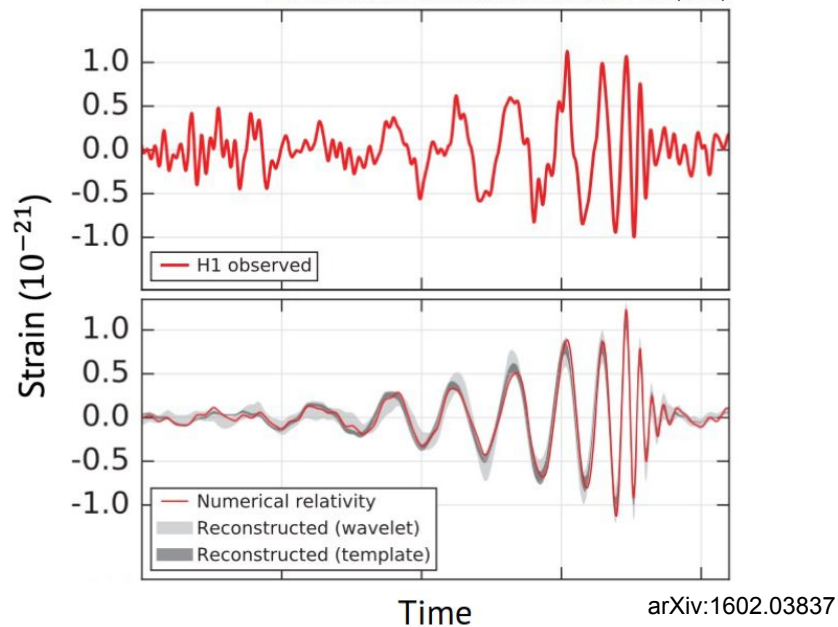


→ Tidal deformabilities

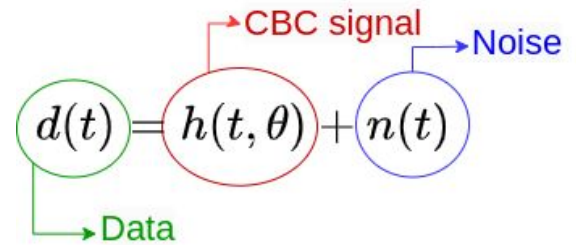
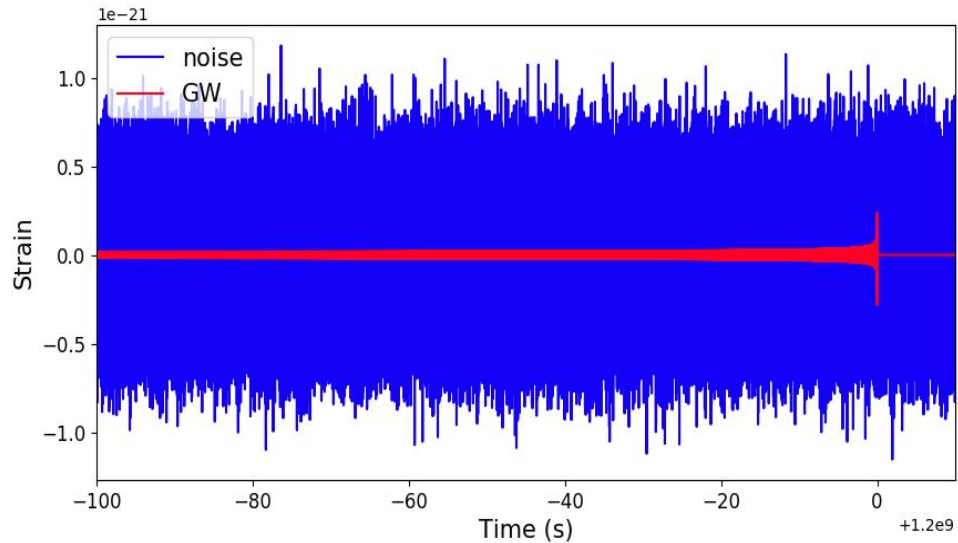


Bayesian analysis

Source characterization from data



Data model



Noise model

→ Stationary noise

- ◆ $\langle n(t) \rangle = \text{cst}$
- ◆ autocorrelation function $R_n(\tau) = \langle n(t) n(t+\tau) \rangle$

Implies that the expected value of the frequency component $\tilde{n}(f)$:

$$\langle \tilde{n}^*(f') \tilde{n}(f) \rangle = \frac{1}{2} S_n(f) \delta(f' - f)$$

with the Power Spectral Density

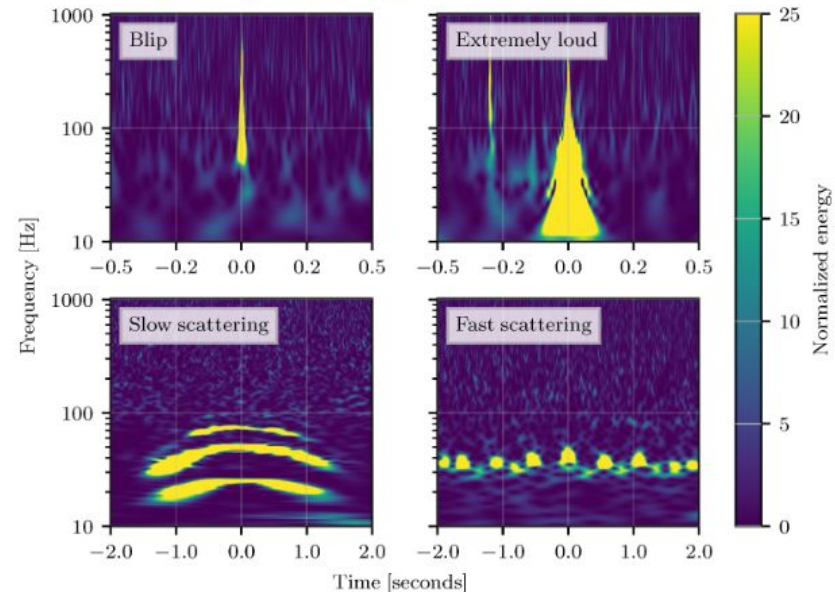
$$S_n(f) = \lim_T \frac{2}{T} \left| \int_{-T/2}^{T/2} n(t) \exp(-2\pi i f t) dt \right|^2$$

→ Gaussian noise distribution

□ The probability density of the time-series $n(t)$ is

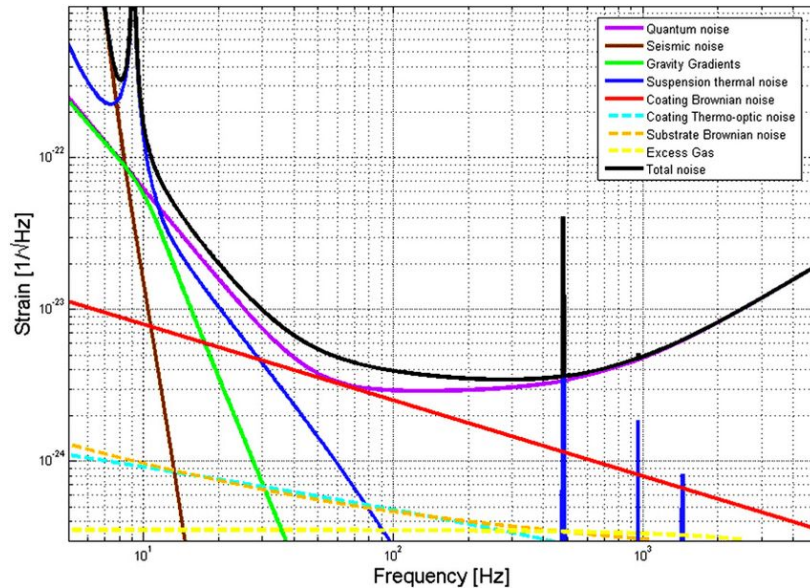
$$p_n[n(t)] \propto \exp \left\{ -\frac{1}{2} 4 \int_0^\infty \frac{|\tilde{n}(f)|^2}{S_n(f)} df \right\}$$

And transient noise!

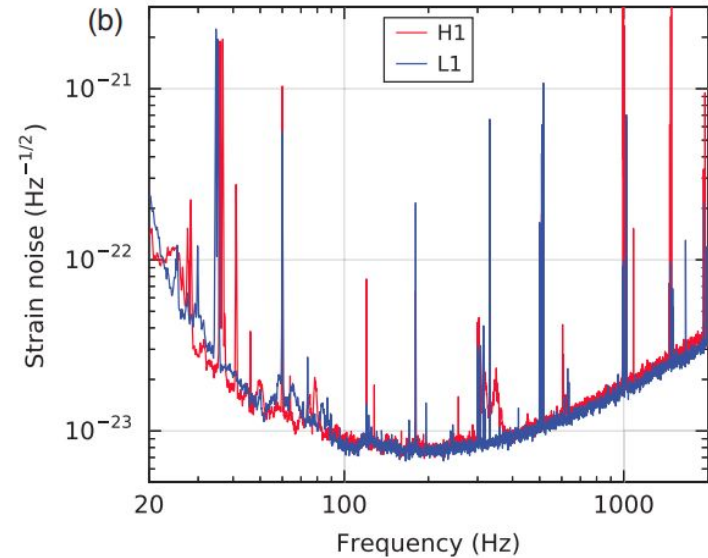


Power Spectral Density

Design noise



Noise during the first event





Likelihood

Likelihood is probability of obtaining data d assuming parameter values θ

$$p(d|\theta) \propto \exp \left\{ -2 \int_0^\infty \frac{|\tilde{n}(f)|^2}{S_n(f)} df \right\} = \exp \left\{ -2 \int_0^\infty \frac{|\tilde{d}(f) - \tilde{h}(f)|^2}{S_n(f)} df \right\}$$

Higher likelihood implies smaller residual.

Bayes' theorem

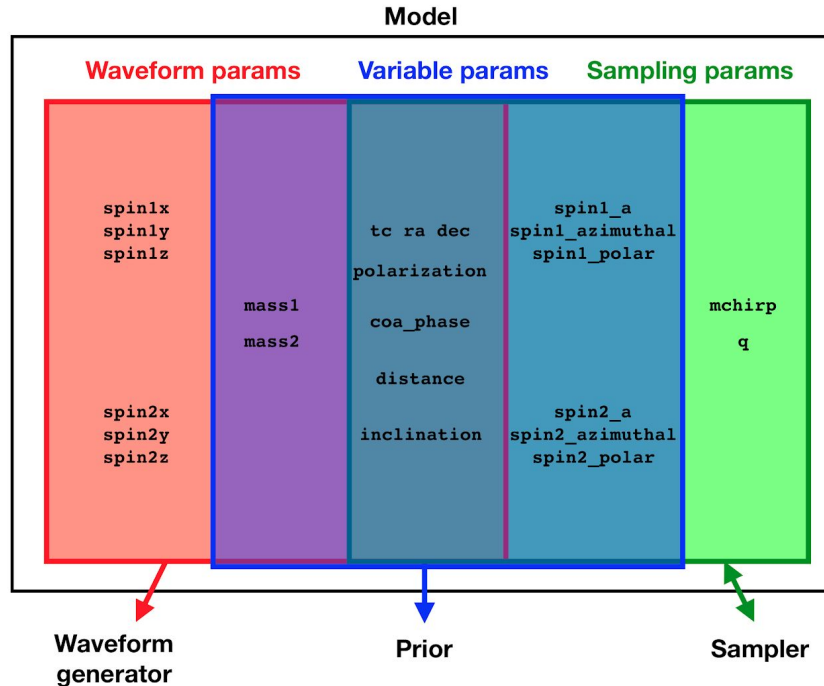
$$P(\mathcal{A}, \mathcal{B}) = P(\mathcal{A})P(\mathcal{B}|\mathcal{A}) = P(\mathcal{B})P(\mathcal{A}|\mathcal{B})$$

$$P(\mathcal{B}|\mathcal{A}) = \frac{P(\mathcal{B})P(\mathcal{A}|\mathcal{B})}{P(\mathcal{A})}$$

$$p(\theta|d, \mathcal{M}_A) = \frac{\pi(\theta|\mathcal{M}_A) \mathcal{L}(d|\theta, \mathcal{M}_A)}{\mathcal{Z}(d|\mathcal{M}_A)}$$

- The **Posterior** distribution is what we want to measure.
- The **Prior** is our prior knowledge on θ
- The **Evidence** is a normalization factor
- The **Likelihood** is calculated from a gravitational waveform, and knowledge of the noise
- The difficulty lies in the fact that these are functions with more than **15 parameters** to study.

Parameter conversion functions



Bilby: a user-friendly Bayesian inference library

- Python codes, installable with pip/conda
- All the components necessary for CBC parameter inference built in (likelihood, priors, parameter conversion functions, ...)
- Supports open-source samplers:
 - ◆ bilby-mcmc
 - ◆ dynesty
 - ◆ ...

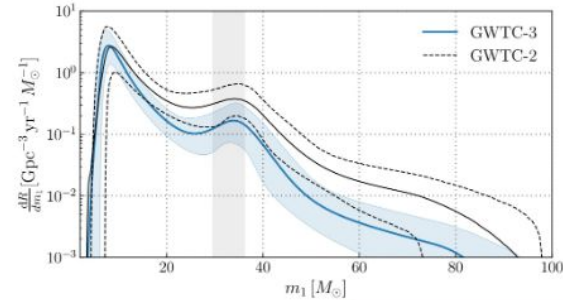


Implications of the CBC observations

Rates and populations

O3a ([arXiv](#)) O3b ([arXiv](#))

- Mass distribution of NS in binaries, different from galactic NS (peak at 1.35 M_{\odot})
- Merger rates depend on models assumed for masses (Power Law + Dip + Break, Binned Gaussian process, Multi source), spins.
- New insight on BH population properties
 - ◆ Mass distribution has a substructure.
 - ◆ Evidence of spin precession, hints of dynamical formation (negative effective spins)
 - ◆ $R_{\text{BBH},z}$ evolution consistent with one of star formation rate



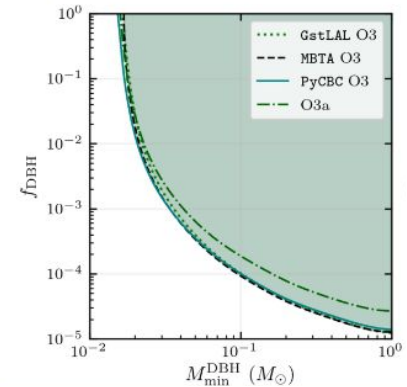
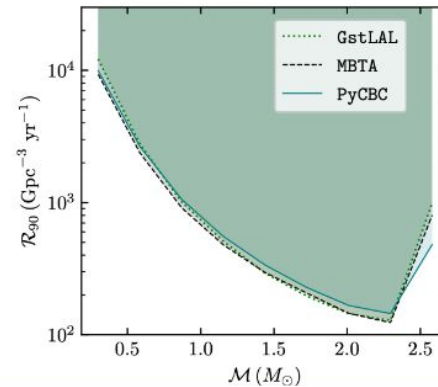
	BNS $m_1 \in [1, 2.5]M_{\odot}$ $m_2 \in [1, 2.5]M_{\odot}$	NSBH $m_1 \in [2.5, 50]M_{\odot}$ $m_2 \in [1, 2.5]M_{\odot}$	BBH $m_1 \in [2.5, 100]M_{\odot}$ $m_2 \in [2.5, 100]M_{\odot}$	NS-Gap $m_1 \in [2.5, 5]M_{\odot}$ $m_2 \in [1, 2.5]M_{\odot}$	BBH-gap $m_1 \in [2.5, 100]M_{\odot}$ $m_2 \in [2.5, 5]M_{\odot}$	Full $m_1 \in [1, 100]M_{\odot}$ $m_2 \in [1, 100]M_{\odot}$
PDB (pair)	170^{+270}_{-120}	27^{+31}_{-17}	$25^{+10}_{-7.0}$	19^{+28}_{-13}	$9.3^{+15.7}_{-7.2}$	240^{+270}_{-140}
PDB (ind)	44^{+96}_{-34}	73^{+67}_{-37}	$22^{+8.0}_{-6.0}$	$12^{+18}_{-9.0}$	$9.7^{+11.3}_{-7.0}$	150^{+170}_{-71}
MS	660^{+1040}_{-530}	49^{+91}_{-38}	37^{+24}_{-13}	$3.7^{+35.3}_{-3.4}$	$0.12^{+24.88}_{-0.12}$	770^{+1030}_{-539}
BGP	$98.0^{+260.0}_{-85.0}$	$32.0^{+62.0}_{-24.0}$	$33.0^{+16.0}_{-10.0}$	$1.7^{+30.0}_{-1.7}$	$5.2^{+12.0}_{-4.1}$	$180.0^{+270.0}_{-110.0}$
MERGED	10 – 1700	7.8 – 140	16 – 61	0.02 – 39	9.4×10^{-5} – 25	72 – 1800

O3 Sub-solar mass

- Sub-solar compact objects predicted by many models:
 - ◆ Primordial Black Holes (BHs) from over densities in early Universe
 - ◆ Dissipative Dark Matter (DM)
 - ◆ BH from DM accumulation in NS cores
- No observation - constraint on the merger rate. Interpretation in two models

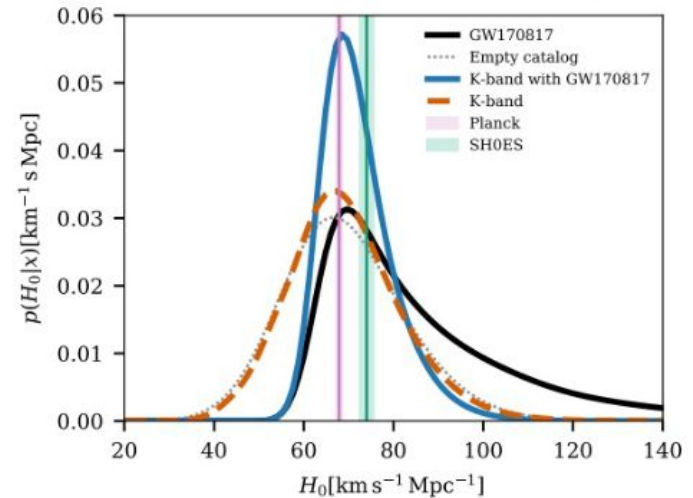


Elisa Nitoglia
Roberto Chierici
Viola Sordini



Cosmology with CBC

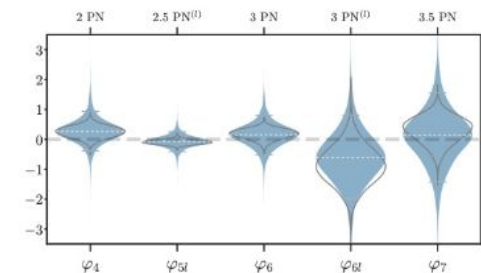
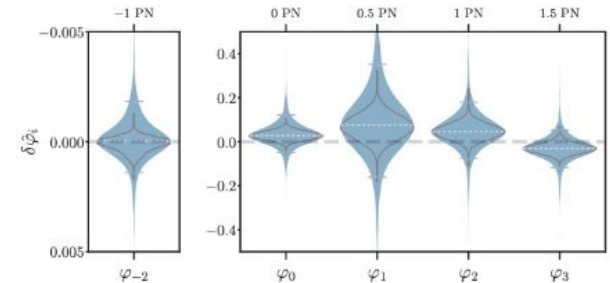
- Based on 47 highly significant ($FAR < 0.25 \text{ yr}^{-1}$, $SNR > 11$) CBC observations: 42 BBH, 2 BNS, 2 NSBH, GW190814
- GW detection implies measuring luminosity distance
- Different methods to constrain H_0
 - ◆ Redshift information from EM counterpart - only for GW170817
 - ◆ Infer the cosmological parameters using statistical galaxy catalog information (use population for out of catalog)
 - ◆ Jointly fitting the cosmological parameters and the source population properties of BBHs



Tests of GR with CBC

- Tests of GR using 47 CBC from GWTC-2 + 15 from GWTC-3 (FAR 10^{-3}/yr) - no evidence for new physics beyond general relativity. Using a large variety of waveform approximants
- Residual tests from remnant coherent power in network data after subtraction of candidates
- Inspiral-merger-ringdown consistency checks (mass and spin of remnant BBH)
- Generic modifications to waveforms (varying post-Newtonian and phenomenological coefficients) à constraints ~2x stronger than previous
- Gravitational-wave dispersion (null in GR) - constraints on Lorentz-violating coefficients, graviton mass $m_g \leq 1.27 \times 10^{-23} \text{ eV}/c^2$ @90%CL
- Data consistent with tensorial polarization, no deviation from Kerr BH, no post-merger echoes

[arXiv](#) & [arXiv](#)



Tidal effects

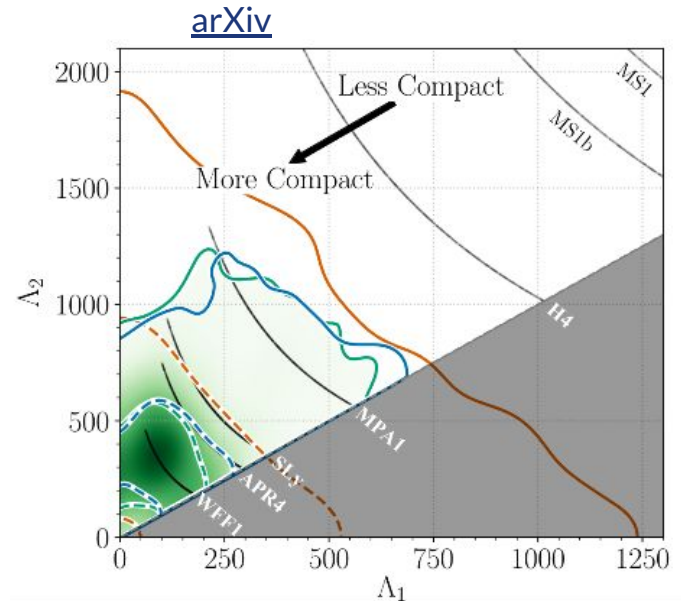
- **Orange** shadow: No relation between the two tidal deformabilities

$$\text{Uniform } \Lambda_2 \in [0, 5000] \quad \text{Uniform } \Lambda_1 \in [0, 5000]$$

- **Green** shadow: EOS-insensitive relation to impose a common EOS for the two bodies

$$\text{Uniform } \Lambda_s \in [0, 5000] \quad \Lambda_a(\Lambda_s, q)$$

- **Blue** shadow: Parametrized EOS expresses the logarithm of the adiabatic index of the EOS $\Gamma(p; \gamma_i)$, as a polynomial of the pressure p , where $\gamma_i = (\gamma_0, \gamma_1, \gamma_2, \gamma_3)$ are the free EOS parameters.



Marginalized posterior for the tidal deformabilities of the two binary components of GW170817 (arXiv:1805.11581)

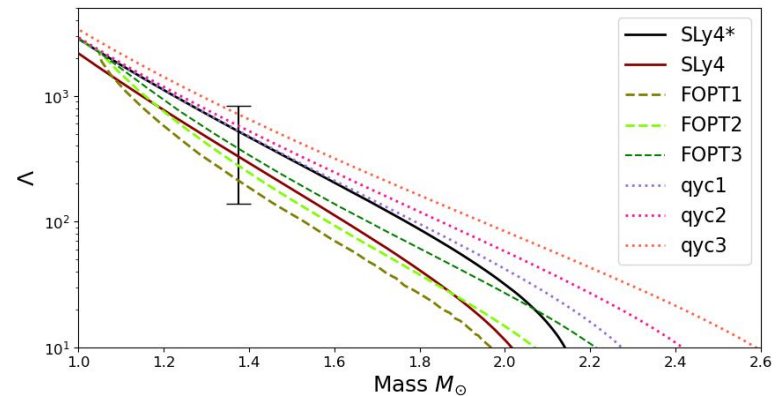
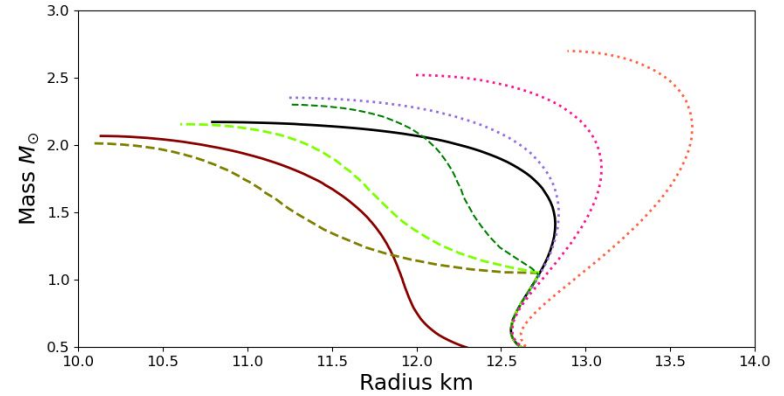
Bayesian inference with fixed equations of state

arXiv:2302.04147

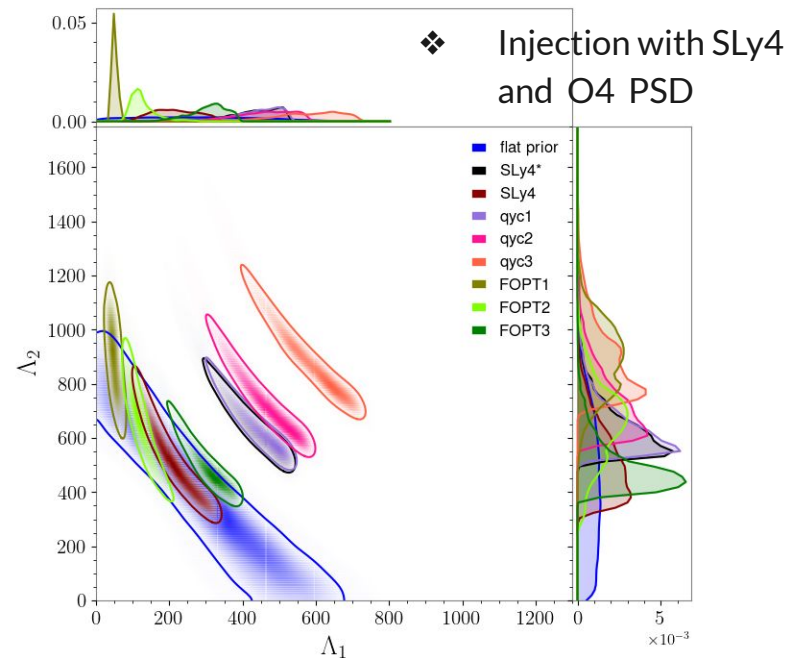
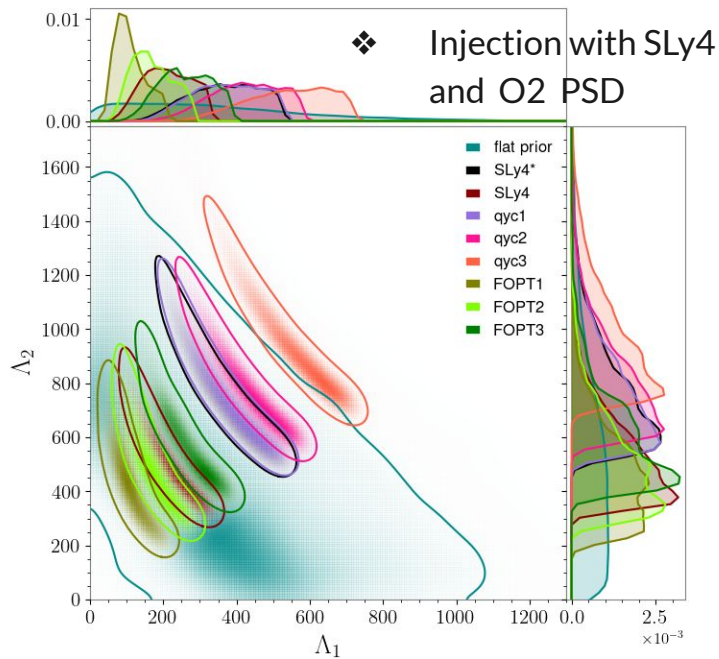
*J-F Coupechoux, R Chierici, H. Hansen,
J. Margueron, R. Somasundaram and V. Sordini*

Equation of state

- ❖ Two nucleonic EOS SLy4 and SLy4*
- ❖ FOPT first order phase transition occurring at $n_t = 2 n_{\text{sat}}$ with the sound speed $c^2 = 2/3$.
- ❖ qyc quarkyonic models adapted to beta-equilibrated matter in compact stars.



Simulated data like GW170817



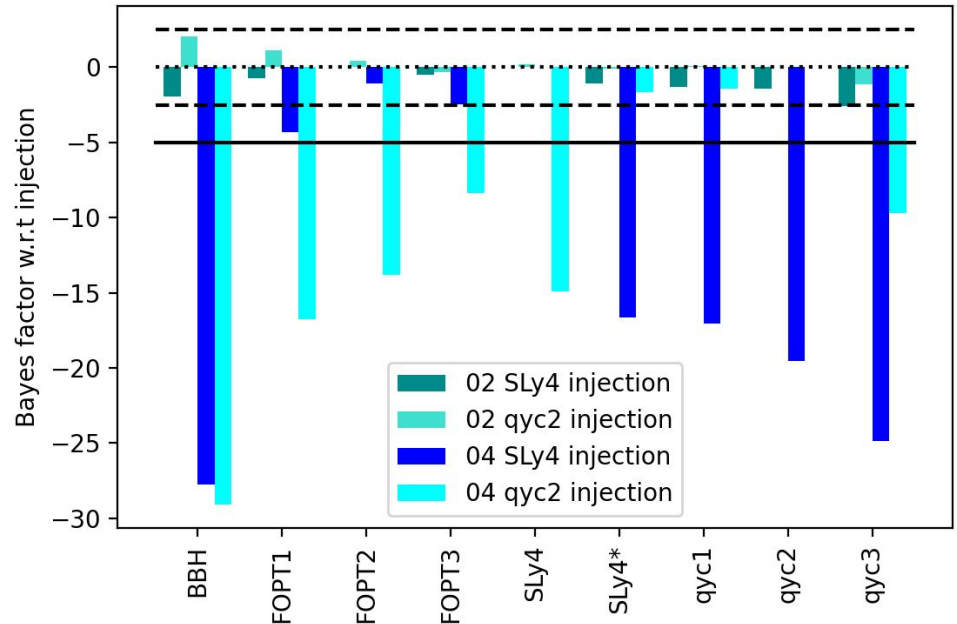
Bayes factor

The Bayes factor defined by

$$\mathcal{B}_{AB} = \frac{Z_A}{Z_B}$$

compare the ability of two models to describe the same data via the Jeffrey's scale.

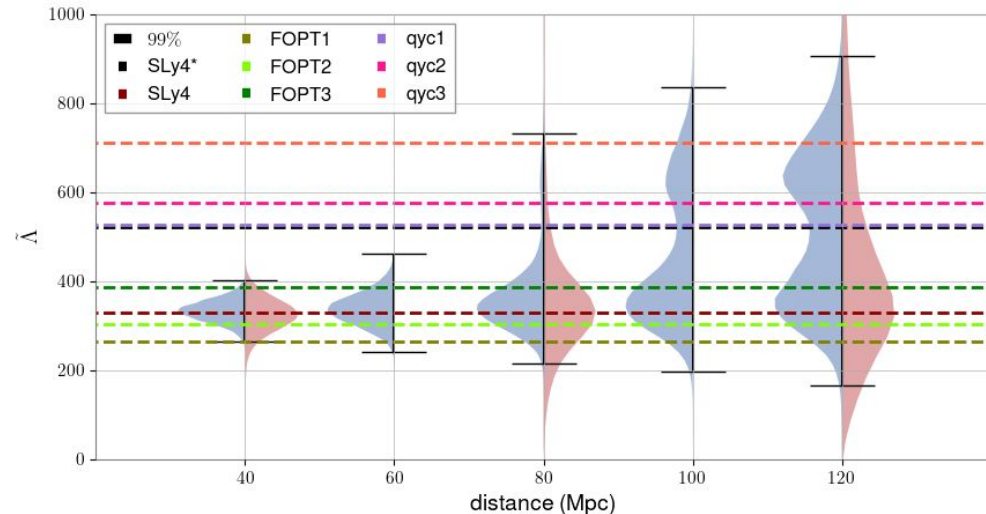
$ \ln \mathcal{B}_{AB} $	Probability	
< 1	< 0.731	Inconclusive
2.5	0.924	Moderate evidence
5	0.993	Strong evidence



Impact of the distance of the source on O4 signal

Impact of the distance on the shape of the reconstructed signal assuming the O4 PSD and SLy4 EoS.

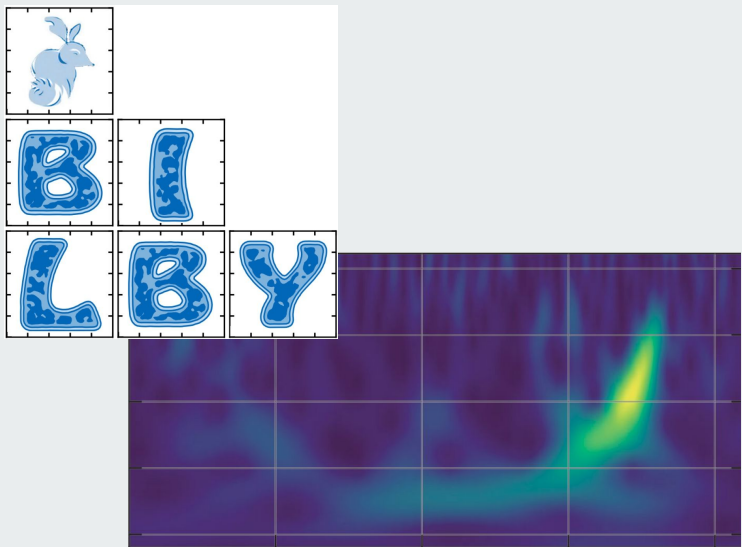
- ❖ The dimensionless effective tidal deformability within an uncertainty 7 times better than the one obtained in O2.
- ❖ Any GW170817-like-single-event within a distance of 100 Mpc would imply significantly improved constraints.
- ❖ The average BNS event rate of having a BNS merger as close as GW170817 is 5-48 years.





PE ROQ runs

Motivation



- ❖ Bayesian inference for a low mass system takes weeks or even months to run with traditional methods.
- ❖ One way to significantly reduce offline parameter estimation run time is using Reduced Order Quadrature (ROQ) rule, see references [1](#), [2](#), and [3](#). This method has been implemented in Bilby package.
- ❖ We expect to have the ROQ method widely used in O4.

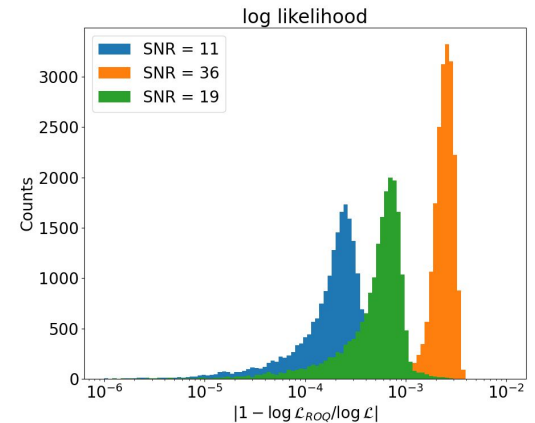
ROQ likelihood vs Standard likelihood

→ $\square \approx [f_{\text{high}} - f_{\text{low}}]$ T terms for the standard likelihood calculation:

$$\begin{aligned}
 & 2 \log \mathcal{L}(d|\vec{\Lambda}) + (d|d) \\
 &= 2\Re \sum_{l=1}^L \frac{4\Delta f \tilde{d}^*(f_l)}{S_n(f_l)} \tilde{h}(f_l; \vec{\Lambda}) - \sum_{l=1}^L \frac{4\Delta f}{S_n(f_l)} \tilde{h}(f_l; \vec{\Lambda}) \tilde{h}^*(f_l; \vec{\Lambda})
 \end{aligned}$$

→ $N_L + N_Q$ terms for the ROQ likelihood calculation:

$$\begin{aligned}
 & 2 \log \mathcal{L}(d|\vec{\Lambda})_{ROQ} + (d|d) \\
 &= 2\Re \sum_{j=1}^{N_L} \omega_j(t_c) \tilde{h}(F_j; \vec{\Lambda}) - \sum_{k=1}^{N_Q} \Psi_k \tilde{h}(\mathcal{F}_k; \vec{\Lambda}) \tilde{h}^*(\mathcal{F}_k; \vec{\Lambda})
 \end{aligned}$$



The likelihoods from the two methods are indistinguishable, up to a tiny fractional difference.

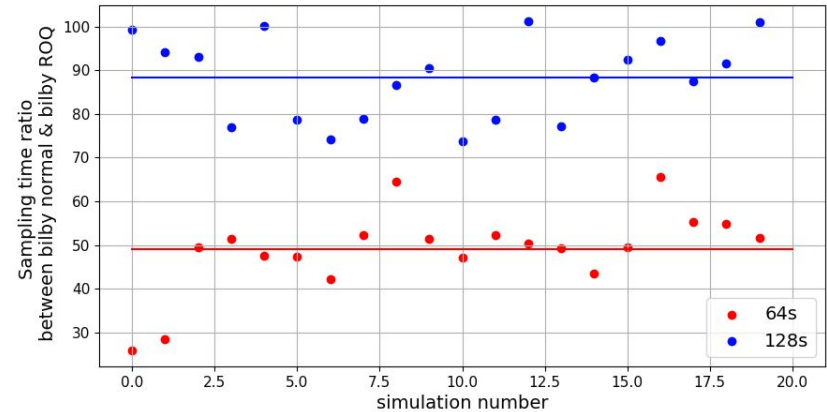
Gains obtained with ROQ: an example

Theoretical gain

Duration	N_L	N_Q	L	Speed up
16s	193	71	32448	123
32s	338	73	64896	158
64s	622	67	129792	188
128s	1156	65	259584	213

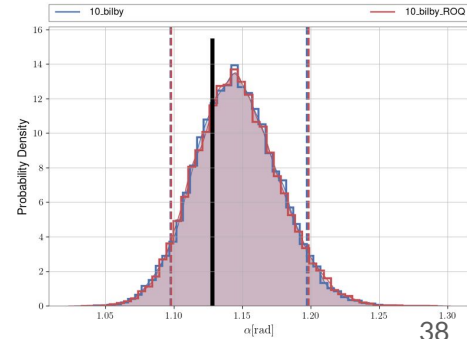
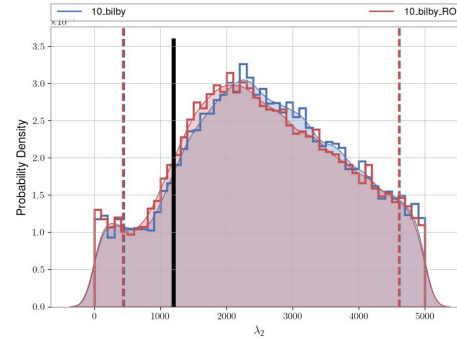
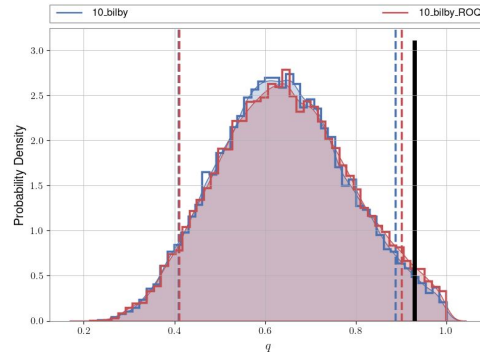
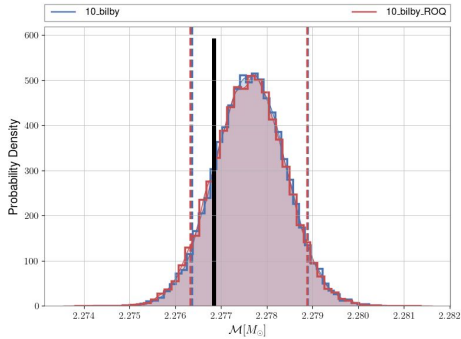
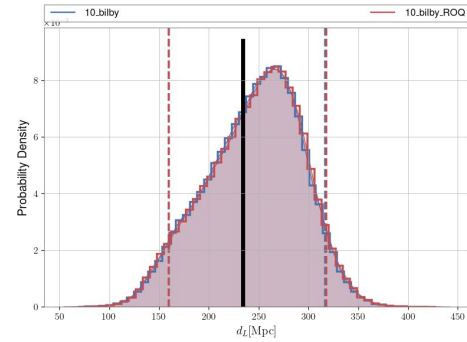
- For a 64s signal, when the sampling time takes 4 hours with ROQ, the standard method takes about 8 days!
- For a 128s signal, when the sampling time takes 6 hours with ROQ, the standard method takes about 23 days!

Gain in practice

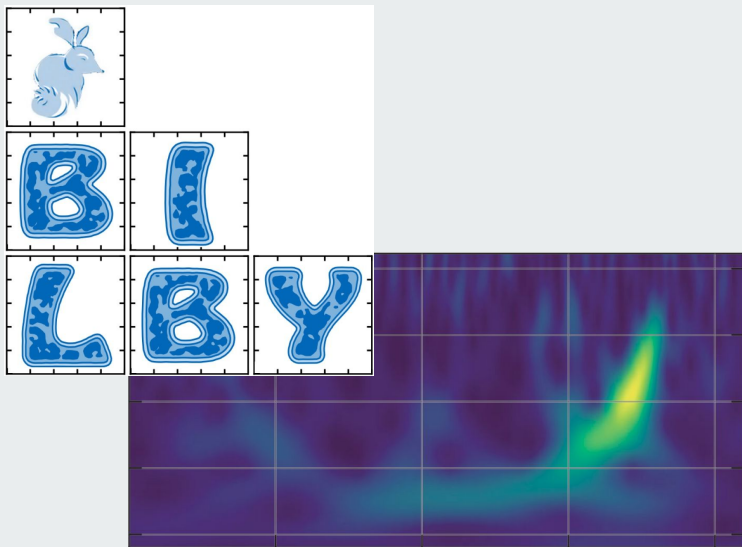


Comparing posteriors

- Optimal SNR = 12.99 for LIGO Hanford; 5.70 for LIGO Livingston and 6.53 for Virgo
- The posteriors are in relatively good agreement.



Summary:



- ❖ ROQ method is:
 - Accurate and reliable
 - Fast
 - Easy to use with Bilby
 - Already available

Inferring Large-scale Simulation of BNS mergers with LVK designed sensitivity

Article in preparation
J-F Coupechoux and H. Qi



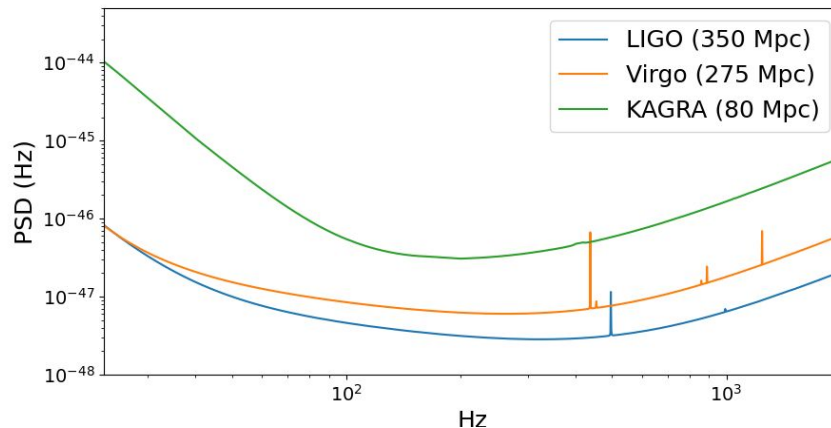
Gains obtained with ROQ

- ❖ The usual technique takes about two days using 160 CPUs with `parallel_bilby`
- ❖ The Bayesian analysis with ROQ takes about two days using only one CPU with `bilby_pipe`

With ROQ, Bayesian analysis of a neutron star merger can be performed during the day.

PE ROQ Robustness Tests with BNS Mergers

- ❖ 10,000 BNS events are simulated using the IMRPhenomPv2_NRTidal approximant.
 - 5,000 using lowspin
 - 5,000 using highspin
- ❖ The waveforms are injected in the LVK collaboration interferometer network.
- ❖ The PSD modeling the detector noise is chosen equal to the expected value for the future run called O5



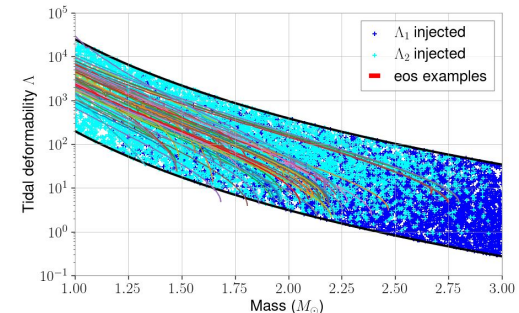
Injected parameters

- ❖ An injection is selected only if single detector SNR > 4 in at least two detectors to do parameter estimation on, i.e., in LVK network.

Parameters θ	Priors $\pi(\theta)$
Masses m_1, m_2	Uniform $m_i \in [1, 3]M_\odot$ with $m_1 > m_2$
Spins $a_1, a_2, \theta_1, \theta_2, \phi_{12}, \phi_{jl}$	Uniform $a_i \in [0, 0.05]$; Sin $\theta_i \in [0, \pi]$; Uniform $\phi_{jl} \in [0, 2\pi]$; Uniform $\phi_{12} \in [0, 2\pi]$
• lowspin	Uniform $a_i \in [0.05, 0.7]$; Sin $\theta_i \in [0, \pi]$; Uniform $\phi_{jl} \in [0, 2\pi]$; Uniform $\phi_{12} \in [0, 2\pi]$
• highspin	Uniform $\alpha \in [0, 2\pi]$; Cos $\delta \in [-\pi/2, \pi/2]$
Sky localization α, δ	Square PowerLaw $d_L \in [10, 460]\text{Mpc}$
Luminosity distance d_L	Uniform $\Psi \in [0, \pi]$; Sin $\theta_{jn} \in [0, \pi]$
Orbital plane Ψ, θ_{jn}	Uniform $\phi_c \in [0, 2\pi]$
Coalescence time ϕ_c	Log Uniform $\Lambda_i \in [200/m_i^6, 25000/m_i^6]$ with $\Lambda_1 < \Lambda_2$
Tidal deformabilities Λ_1, Λ_2	

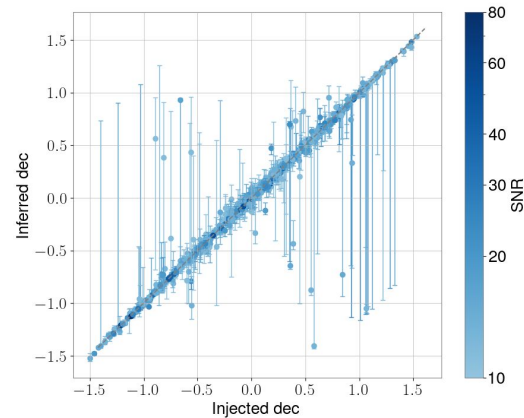
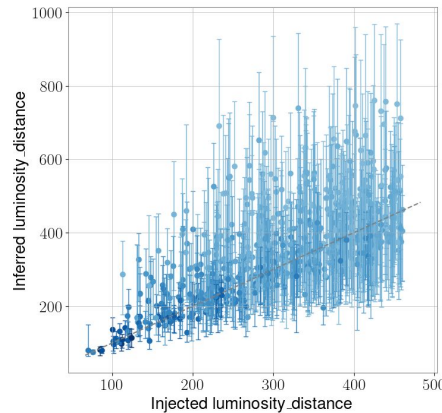
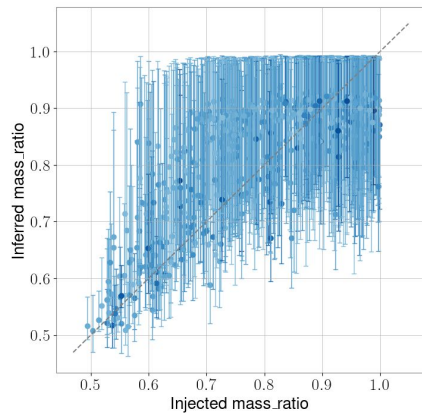
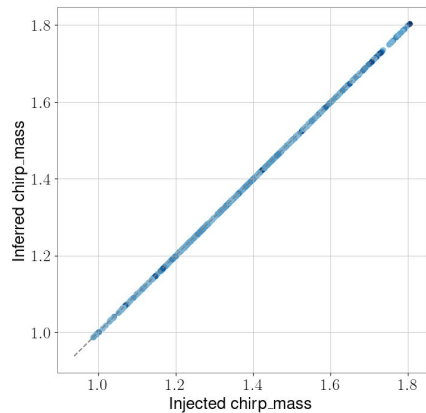
- ❖ This selection has three major effects:
 - a decrease of the number of injection for low masses
 - a decrease of injection at long distance
 - a decrease of injection with the merge plane orthogonal to the direction of observation.

TABLE I. Probability distribution used to create BNS injections.



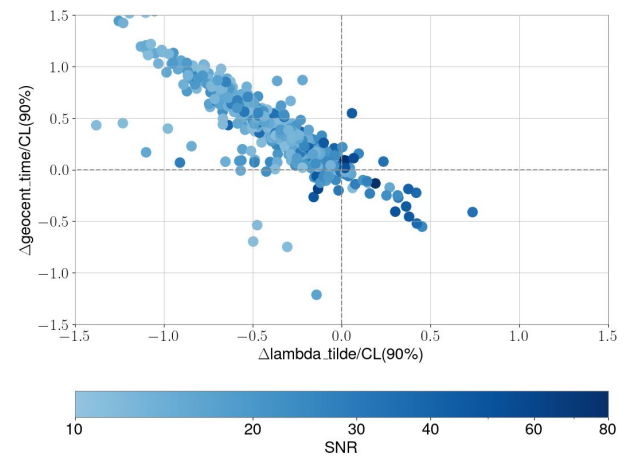
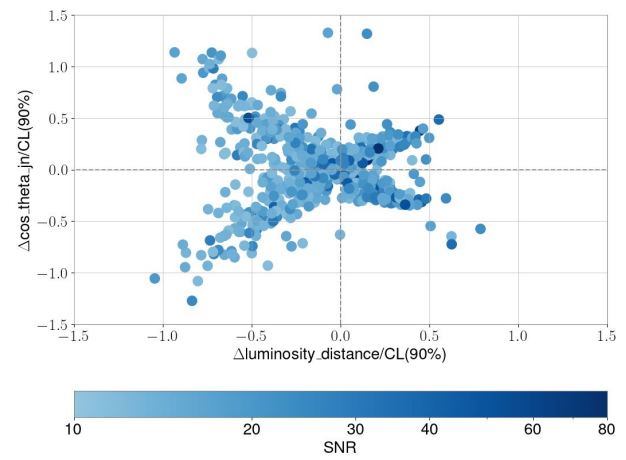
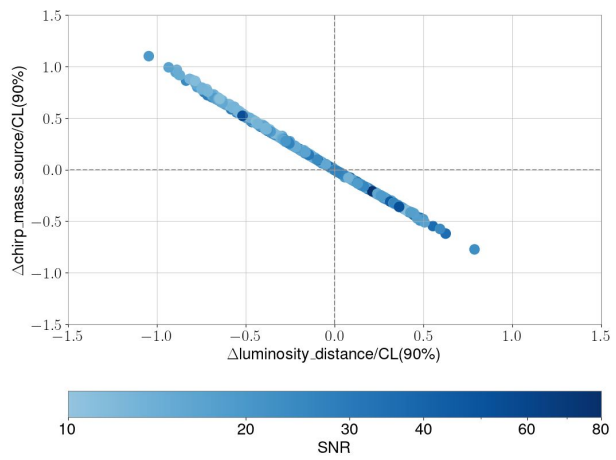


Inferred and injected parameters





Bias plots



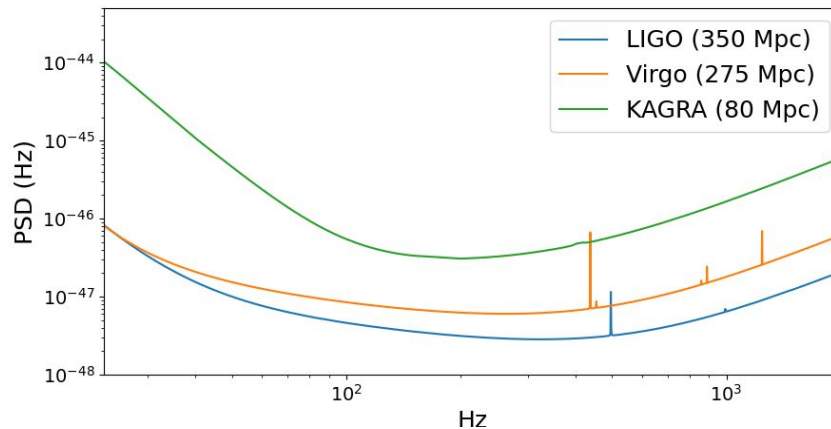
Measuring Neutron Star Equation of State with LVK

Article in preparation

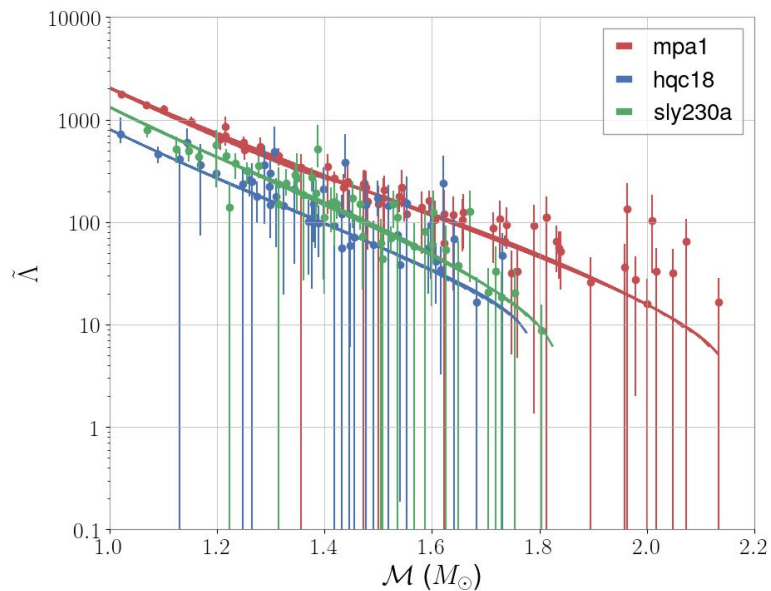
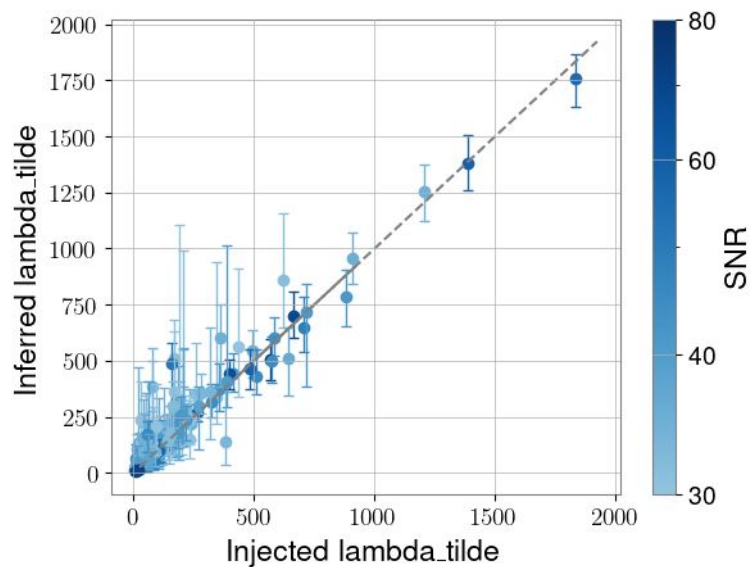
J-F Coupechoux, P. Landry and H. Qi

PE ROQ Robustness Tests with BNS Mergers

- ❖ 3000 BNS events are simulated using the IMRPhenomPv2_NRTidal approximant.
 - 1000 using mpa1 eos
 - 1000 using sly230a eos
 - 1000 using hqc18 eos
- ❖ The waveforms are injected in the LVK collaboration interferometer network.
- ❖ The PSD modeling the detector noise is chosen equal to the expected value for the future run called O5



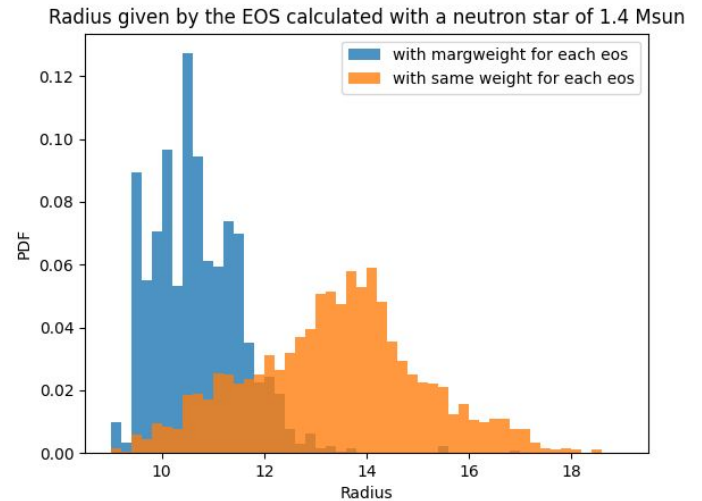
Effective tidal deformability



→ Among the 3000 injections only 146 have a SNR higher than 30

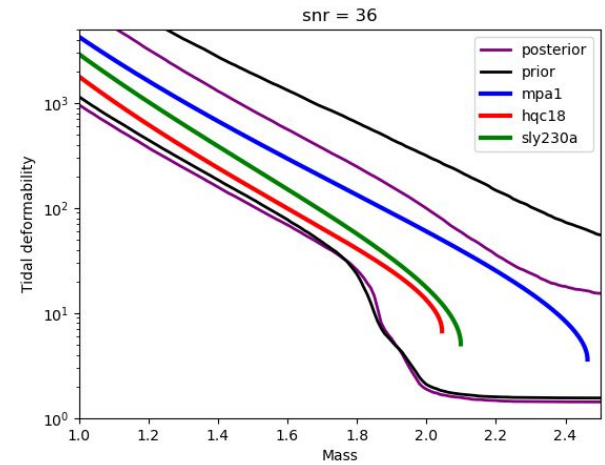
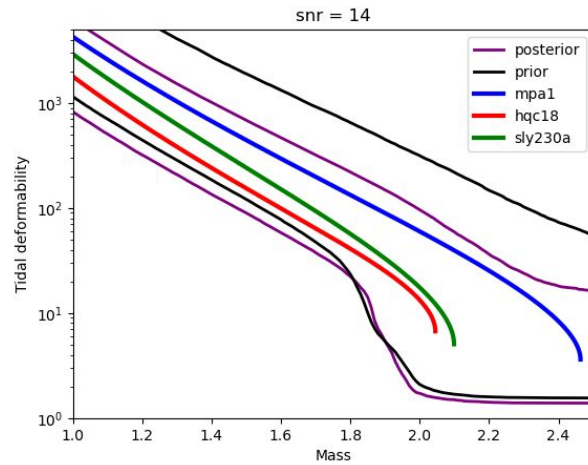
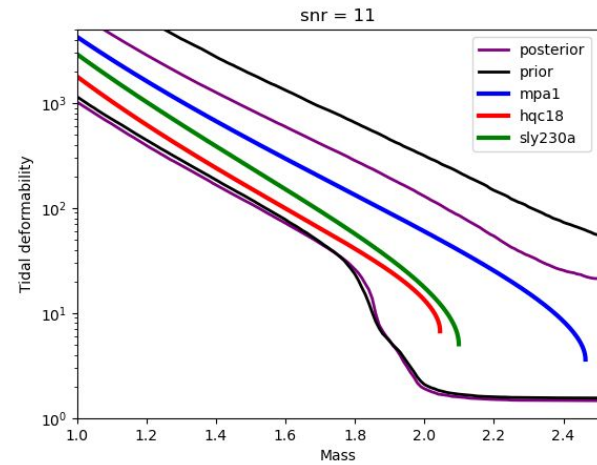
Nonparametric inference of neutron star composition

- Compute marginal likelihoods for GW data given a set of candidate equations of state.
- This is done through Monte Carlo sampling from a prior defined over component masses, tidal deformabilities in combination with a likelihood model constructed from a Gaussian kernel density estimate.
- A probability is associated with each equation of state.

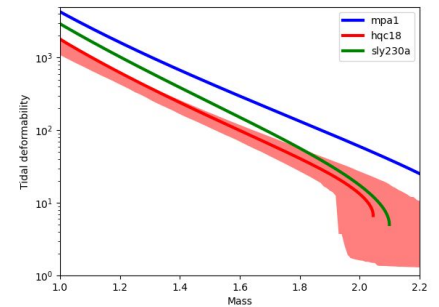
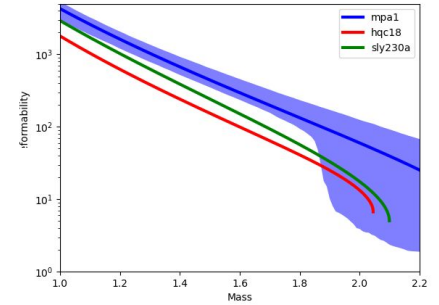
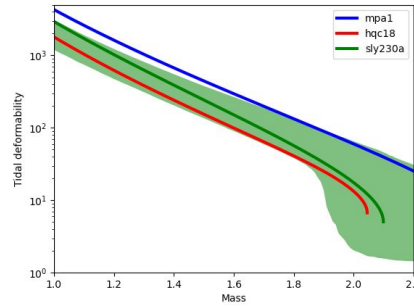
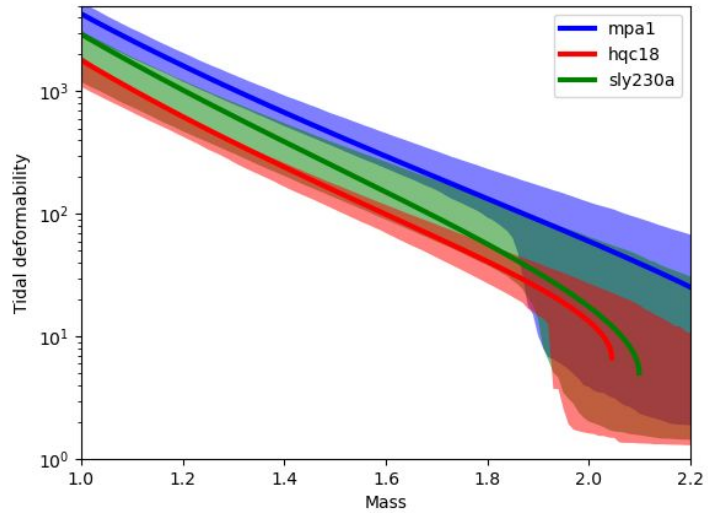




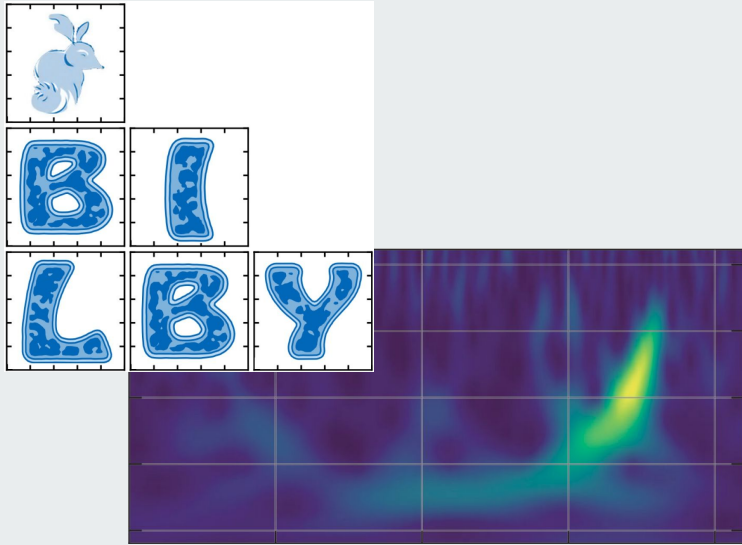
Measuring the equation of state of simulated events



Combination of 10 events



Summary:

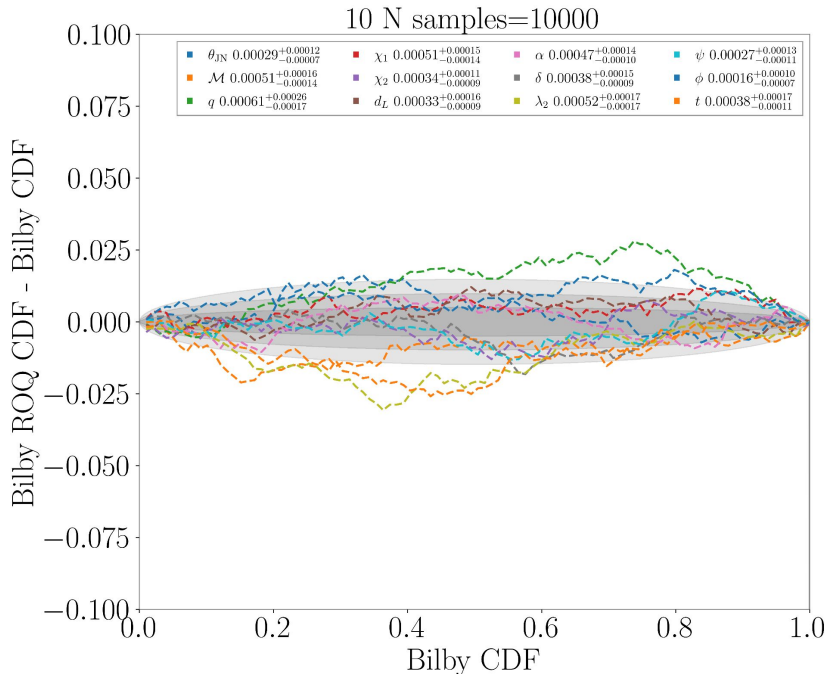


- ❖ To finish
 - Spectral representations of neutron-star equation of state
 - Comparison between direct and a posteriori estimation
- ❖ ROQ method is
 - Accurate and reliable
 - Fast
 - Easy to use with Bilby
 - Already available



Thank you for your attention

Jensen-Shannon divergence



- Difference between samples recovered by Bilby ROQ and Bilby for all parameters.
- Labels show the mean Jensen-Shannon (JS) divergence between Bilby ROQ and Bilby normal for all parameters, evaluated by random re-sampling over 100 iterations.
- The JS divergence value must be greater than 0.002 to talk about statistically significant.